Activation of the nuclear receptor FXR improves hyperglycemia and hyperlipidemia in diabetic mice

Yanqiao Zhang*†, Florence Ying Lee*†, Gabriel Barrera*†, Hans Lee*†, Charisse Vales†, Frank J. Gonzalez‡, Timothy M. Willson§, and Peter A. Edwards*†¶‖

*Department of Biological Chemistry, CHS 33-257, 10833 Le Conte Avenue, University of California, Los Angeles, CA 90095; †Department of Medicine and ¶Molecular Biology Institute, University of California, Los Angeles, CA 90095; ‡Laboratory of Metabolism, National Cancer Institute, National Institutes of Health, Bethesda, MD 20892; and §Discovery Research, GlaxoSmithKline, Research Triangle Park, NC 27709

Edited by Richard J. Havel, University of California School of Medicine, San Francisco, CA, and approved November 29, 2005 (received for review August 11, 2005)

Farnesoid X receptor (FXR) plays an important role in maintaining bile acid and cholesterol homeostasis. Here we demonstrate that FXR also regulates glucose metabolism. Activation of FXR by the synthetic agonist GW4064 or hepatic overexpression of constitutively active FXR by adenovirus-mediated gene transfer significantly lowered blood glucose levels in both diabetic db/db and wild-type mice. Consistent with these data, FXR null mice exhibited glucose intolerance and insulin insensitivity. We further demonstrate that activation of FXR in db/db mice repressed hepatic gluconeogenic genes and increased hepatic glycogen synthesis and glycogen content by a mechanism that involves enhanced insulin sensitivity. In view of its central roles in coordinating regulation of both glucose and lipid metabolism, we propose that FXR agonists are promising therapeutic agents for treatment of diabetes mellitus.

glucose | GW4064 | farnesoid X receptor-VP16 | triglyceride | cholesterol

Diabetes mellitus is associated with a 2- to 4-fold increase in the risk of coronary artery disease (1, 2) and is one of the leading causes of morbidity and mortality in the United States. Numerous studies have demonstrated that the control of blood glucose levels is critical for either preventing or delaying the progression of clinical complications of diabetes (3, 4). Liver plays an essential role in the control of blood glucose levels by modulating gluconeogenesis and glycogen synthesis (5). Phosphoenolpyruvate carboxykinase (PEPCK) catalyzes the initial step of gluconeogenesis, whereas glucose-6-phosphatase (G6Pase) catalyzes the last committed step of this process. Hence, overexpression of G6Pase increases glucose production and causes hyperglycemia and glucose intolerance (6). The expression of both PEPCK and G6Pase is primarily regulated at the level of transcription (7). In contrast, glycogen synthase, the rate-limiting enzyme of glycogen biosynthesis (8), is regulated posttranscriptionally by glycogen synthase kinase 3β (GSK3β) (9).

Farnesoid X receptor (FXR) is a member of the nuclear hormone receptor superfamily. High expression of FXR is limited to the liver, intestine, kidney, and adrenal gland (10–12). Studies using FXR$^{-/-}$ mice and FXR agonists have demonstrated a critical role for FXR in maintaining cholesterol and bile acid homeostasis as a result of the regulation of hepatic genes controlling both the catabolism of cholesterol to bile acids and the subsequent secretion of bile acids into the bile (13–16). In addition, activation of FXR lowers plasma triglyceride levels (15, 17) by a mechanism that involves the repression of hepatic SREBP-1c expression (18, 19).

Herein, we demonstrate that transfusion of wild-type, FXR$^{-/-}$, or diabetic db/db mice with adenovirus expressing constitutively active FXR lowers blood glucose and lipid levels. Treatment of wild-type or db/db mice, but not FXR$^{-/-}$ mice, with a highly specific synthetic FXR agonist also decreased plasma glucose and lipid levels. These results reveal a previously uncharacterized role for FXR in controlling glucose homeostasis.

Results

Activation of FXR by GW4064 Lowers Plasma Glucose Levels in Wild-Type Mice. Analysis of microarray data from a screen designed to identify FXR target genes suggested that FXR regulated genes involved in gluconeogenesis (data not shown). In an attempt to determine the role of FXR in glucose homeostasis, murine primary hepatocytes were treated with either vehicle or the FXR agonist GW4064 for 24 h. Treatment with GW4064 induced both small heterodimer parter (SHP), a well characterized FXR target gene (20, 21), and PEPCK (Fig. 1*A*). However, GW4064 treatment led to repression of G6Pase mRNA levels (Fig. 1*A*), suggesting that activation of FXR may affect gluconeogenesis.

To investigate whether activation of FXR *in vivo* by GW4064 regulated plasma glucose levels, we gavaged wild-type and FXR$^{-/-}$ mice daily with GW4064 for 11 days. Data from real-time PCR revealed that GW4064 treatment induced hepatic mRNA levels of small heterodimer parter (SHP), PEPCK, and scavenger receptor class B, type I (SR-BI) in wild-type but not FXR$^{-/-}$ mice (Fig. 1*B*). SR-BI is known to facilitate the clearance of HDL cholesterol from blood (22). Because overexpression of SR-BI in the liver is associated with reduced plasma HDL levels (23), we hypothesize that the decline in plasma cholesterol levels (Fig. 1*E*) results, at least in part, from the induction of hepatic SR-BI. GW4064 treatment also significantly lowered hepatic G6Pase and SREBP-1c mRNA levels by an FXR-dependent process (Fig. 1*B*). We and others have previously proposed that the repression of SREBP-1c by GW4064 results in reduced hepatic triglyceride synthesis and plasma triglyceride levels (18, 19).

Consistent with the repression of hepatic G6Pase mRNA levels, plasma glucose levels were significantly decreased in wild-type mice after 4 days (Fig. 7, which is published as supporting information on the PNAS web site) or 11 days (Fig. 1*C*) treatment with GW4064. In contrast, glucose levels did not decrease when FXR$^{-/-}$ mice were treated with GW4064 (Figs. 1*C* and 7). Plasma triglyceride and cholesterol levels were also significantly decreased in GW4064-treated wild-type but not FXR$^{-/-}$ mice (Fig. 1 *D* and *E*). We conclude that administration of GW4064 to mice results in a reduction in plasma glucose, triglyceride, and cholesterol levels by mechanisms that require FXR.

The FXR Agonist GW4064 Significantly Improves Hyperglycemia and Hyperlipidemia in Diabetic db/db Mice. The finding that activation of FXR lowered plasma glucose levels in nondiabetic mice prompted us to investigate the role of FXR in a diabetic mouse model. The db/db mice lack functional leptin receptors and have been extensively studied as a model for type 2 diabetes (24, 25). Diabetic db/db mice and their lean littermates were treated with vehicle or GW4064 for 5 days. GW4064 treatment had no effect on food intake, liver weight, or weight gain (data not shown). As

Conflict of interest statement: No conflicts declared.

This paper was submitted directly (Track II) to the PNAS office.

Abbreviations: FXR, farnesoid X receptor; G6Pase, glucose-6-phosphatase; GSK3β, glycogen synthase kinase 3β; IRS, insulin receptor substrate; PEPCK, phosphoenolpyruvate carboxykinase; SR-BI, scavenger receptor class B, type 1.

‖To whom correspondence should be addressed. E-mail: pedwards@mednet.ucla.edu.

www.pnas.org/cgi/doi/10.1073/pnas.0506982103

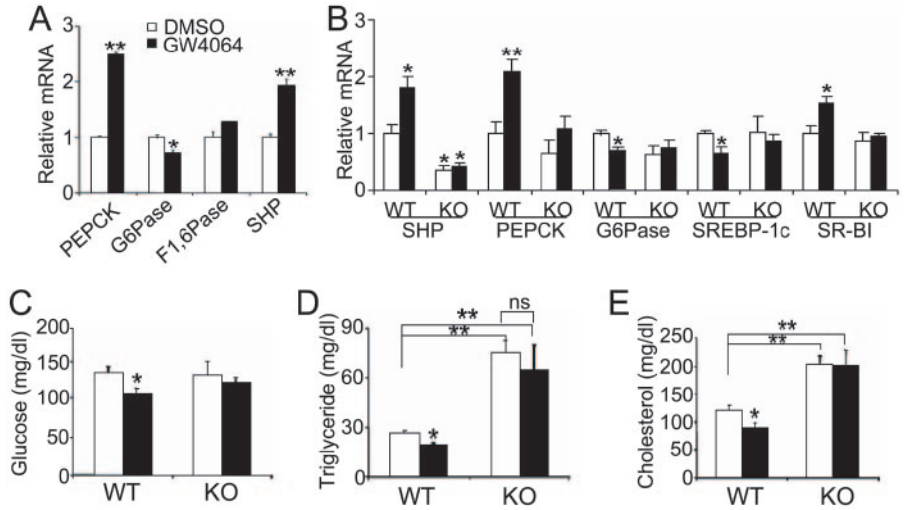

Fig. 1. The FXR agonist GW4064 regulates glucose and lipid homeostasis in an FXR-dependent manner. (*A*) Murine primary hepatocytes were treated with either vehicle (DMSO) or GW4064 (1 μM) for 24 h. mRNA levels were quantified by real-time PCR and normalized to cyclophilin. F1,6Pase, fructose 1,6-bis phosphatase. (*B–E*) Wild-type and FXR$^{-/-}$ mice were gavaged with either vehicle (open bars) or GW4064 (filled bars) for 11 days ($n = 6$ per group). After a 6-h fast, livers were removed and hepatic mRNA levels were quantified by real-time PCR (*B*). Plasma glucose (*C*), triglyceride (*D*), and cholesterol (*E*) levels were determined after a 6-h fast. *, $P < 0.05$. **, $P < 0.01$ versus control (*A* and *C–E*) or vehicle-treated wild-type group (*B*), unless specifically indicated.

expected, compared to their lean littermates, chow-fed db/db mice had markedly enhanced plasma levels of glucose, β-hydroxybutyrate, triglycerides, free fatty acids, and cholesterol (Fig. 2 *A–E*). Treatment of db/db mice with GW4064 significantly reduced the plasma levels of all these metabolites (Fig. 2 *A–E*). Importantly, these values approached those of the lean, untreated littermates (Fig. 2 *A–E*).

Hematoxylin and eosin (H&E) and oil red O staining indicated that GW4064 treatment significantly reduced neutral lipid accumulation in the livers of db/db mice (Fig. 2*F*). Collectively, these data demonstrate that activation of FXR by GW4064 markedly reduces hepatic neutral lipid levels and improves both hyperglycemia and the plasma lipid profile of diabetic db/db mice.

To assess whether gene expression of db/db mice was affected by GW4064 treatment, we analyzed selected hepatic genes. As shown in Fig. 2*G*, db/db mice had elevated hepatic mRNA levels of FXRα1+α2 and FXRα3+α4 compared to their lean littermates. The increase in hepatic FXR mRNA levels is consistent with *in vitro* studies that demonstrated that FXR mRNA levels increased when rat primary hepatocytes were exposed to high glucose levels (26).

The data of Fig. 2*G* demonstrate that GW4064 treatment significantly repressed hepatic G6Pase and PEPCK mRNA levels in db/db mice. This effect was specific because glucose transporter 2 (Glut2) mRNA levels were unchanged (Fig. 2*G*). However, the suppression of PEPCK mRNA levels by GW4064 in db/db mice was surprising because GW4064 treatment induced PEPCK expression in wild-type C57BL/6 mice or isolated hepatocytes (Fig. 1 *A* and *B*). Nonetheless, the data of Fig. 2*G* suggest that GW4064 treatment of db/db mice suppressed two important hepatic gluconeogenic genes.

GW4064 Increases Hepatic Glycogen Synthesis and Storage in db/db Mice. Hepatic glycogen synthesis and breakdown play an important role in modulating blood glucose levels (27). Accordingly, the effect of GW4064 on hepatic glycogen levels was determined by using periodic acid-Schiff staining and colorimetric assay. As shown in

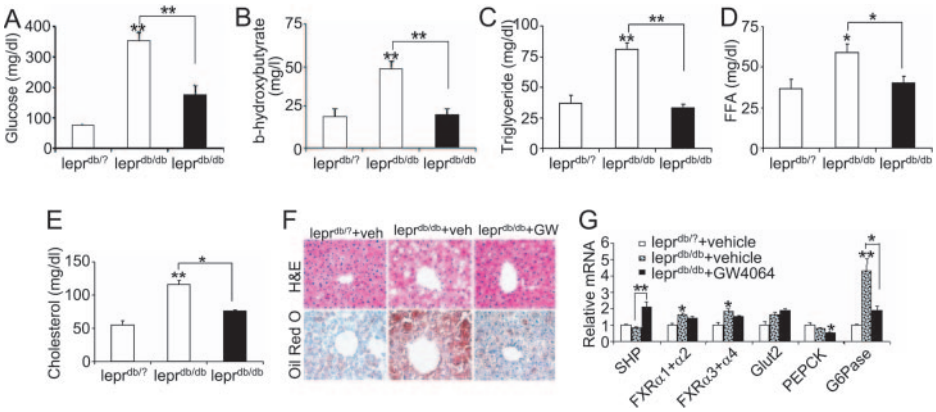

Fig. 2. GW4064 treatment of db/db mice results in hypoglycemia and hypolipidemia. (*A–F*) Eighteen-week-old female lepr$^{db/db}$ mice ($n = 6$ for vehicle-treated group, $n = 5$ for GW4064-treated group) and their lean littermates Lepr$^{db/?}$ ($n = 4$) were treated daily with either vehicle (open bars) or GW4064 (filled bars) for 5 days. After a 16-h fast, plasma levels of glucose (*A*), β-hydroxybutyrate (*B*), triglyceride (*C*), free fatty acids (FFA) (*D*), and total cholesterol (*E*) were determined. (*F*) Liver sections were stained with hematoxylin/eosin (H&E) (*Upper*) or oil red O (*Lower*). (Magnification: ×400.) (*G*) Determination of hepatic mRNA levels by real-time PCR. Glut2, glucose transporter 2. *, $P < 0.05$. **, $P < 0.01$ versus lepr$^{db/?}$ mice unless specifically indicated.

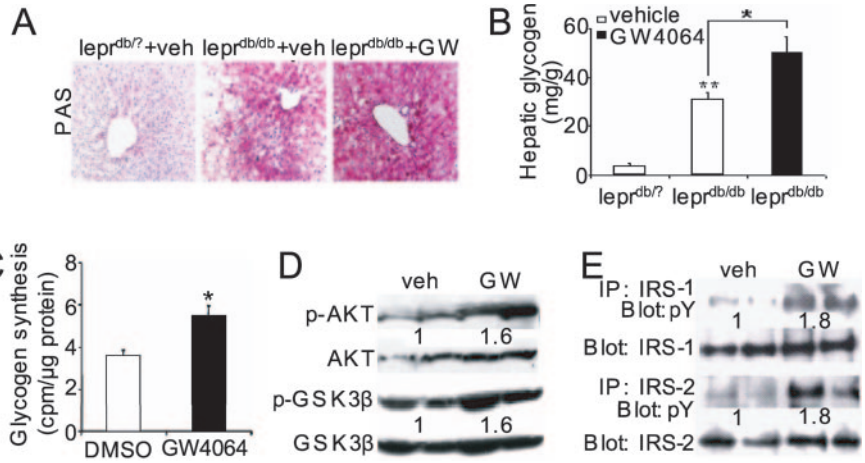

Fig. 3. GW4064 treatment enhances insulin signaling and glycogen storage in the livers of db/db mice. Mice were treated with GW4064 for 5 days (*A*, *B*, *D*, and *E*). (*A* and *B*) Hepatic glycogen levels were determined by periodic acid-Schiff staining (*A*) or colorimetric assay (*B*). (Magnification: *A*, ×200.) (*C*) Murine primary hepatocytes were treated in triplicate with DMSO or GW4064 (1 μM) for 24 h, followed by incubation with media containing ^{14}C-D-glucose for 2 h. The incorporation of ^{14}C-D-glucose into glycogen was quantified. (*D*) Determination of phosphorylation levels of hepatic Akt and GSK3β in db/db mice. (*E*) Determination of phosphotyrosine (pY) levels of hepatic IRS-1 or IRS-2 in db/db mice. *, $P < 0.05$. **, $P < 0.01$ versus vehicle-treated primary hepatocytes or lepr$^{db/?}$ mice unless specifically indicated.

Fig. 3 *A* and *B*, db/db mice had elevated hepatic glycogen levels as compared to their lean littermates. In addition, hepatic glycogen levels were further increased after treatment of db/db mice with GW4064 (Fig. 3 *A* and *B*). Finally, treatment of primary hepatocytes with GW4064 was shown to increase the incorporation of ^{14}C-D-glucose into glycogen (Fig. 3*C*). Taken together, these data demonstrate that the FXR agonist GW4064 increases hepatic glycogen synthesis and storage.

Nonphosphorylated GSK3β is constitutively active and represses glycogen synthase activity (28). Importantly, GW4064 treatment of db/db mice increased the hepatic levels of phosphorylated GSK3β (at Ser-9) (Fig. 3*D*). Because the phosphorylation of GSK3β at Ser-9 is known to increase glycogen synthase activity (29) and the decreased G6Pase mRNA levels (Fig. 2*G*) may also lead to increased glycogen synthesis, these data provide a mechanism by which activated FXR increases glycogen levels in the liver.

It has been well established that insulin represses hepatic gluconeogensis and increases glycogen synthesis (27). The effect of GW4064 on glucose homeostasis in db/db mice is reminiscent of insulin action. In addition to phosphorylating GSK3β (30), insulin is known to induce the phosphorylation of insulin receptor substrate (IRS) 1, IRS-2, and Akt (27, 31). Consequently, we investigated the effect of GW4064 treatment on the phosphorylated levels of IRS-1, IRS-2, and Akt; the data show that GW4064 treatment of db/db mice significantly increased hepatic levels of phosphorylated IRS-1 and IRS-2 (Fig. 3*E*) and phosphorylated Akt (Fig. 3*D*). Collectively, these data demonstrate that activation of FXR by GW4064 increases hepatic glycogen storage likely through increased insulin sensitivity.

Hepatic Overexpression of Constitutively Active FXR Lowers Plasma Glucose Levels in Nondiabetic Mice. To better understand the physiological role of activated hepatic FXR, we generated adenovirus expressing VP16 (Ad-VP16), the transactivation domain of herpes simplex virus, or murine FXRα2 fused to VP16 (Ad-FXRα2-VP16). Importantly, FXR-VP16 is constitutively active in the absence of an FXR agonist.

Either Ad-VP16 or Ad-FXRα2-VP16 was transfused into the tail veins of wild-type C57BL/6J mice. Numerous studies have demonstrated that infusion of adenovirus by tail vain injection results in overexpression of genes that are essentially limited to the liver. Hepatic expression of FXRα2-VP16 did not affect the expression of endogenous FXR mRNA but did lead to a significant induction of the FXR target gene small heterodimer parter (SHP) (Fig. 4*A*). Thus, FXRα2-VP16 was functionally active in the livers of these C57BL/6J mice. FXRα2-VP16 expression also lowered plasma cholesterol and glucose levels (Fig. 4 *B* and *C*), consistent with a critical role for FXR in controlling plasma lipid and glucose levels. As expected, transfusion of adenovirus expressing VP16 *per se* had no effect on plasma glucose levels compared to uninfected wild-type mice (Fig. 4*C*). To better understand the physiological role of activated FXR and avoid any confounding effect from the endogenous murine FXRs, adenovirus was also transfused into FXR$^{-/-}$ mice (Fig. 4*D*); the data show that blood glucose levels of FXR$^{-/-}$ mice were reduced significantly after transfusion of FXRα2-VP16. Taken together, these data demonstrate that hepatic overexpression of constitutively active murine FXR lowers plasma glucose and lipid levels.

Hepatic Overexpression of Constitutively Active FXR Significantly Improves Hyperglycemia in db/db Mice. Oral administration of GW4064 activates both intestinal and hepatic FXR. To investigate

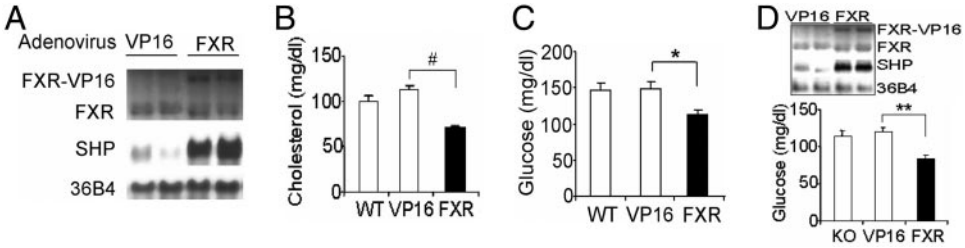

Fig. 4. Hepatic expression of FXR-VP16 decreases plasma glucose and cholesterol levels in nondiabetic mice. (*A–C*) C57BL/6J mice were separately transfused with Ad-VP16 (VP16) or Ad-FXR-VP16 (FXR) or saline alone (WT) by tail vain injection ($n = 8$ per group). After 7 days, mice were fasted for 6 h before being killed. Hepatic mRNA levels were quantified by Northern blot assay (*A*), and plasma cholesterol (*B*) and glucose (*C*) levels were determined. (*D*) Hepatic expression of FXRα2-VP16 lowers plasma glucose levels in FXR$^{-/-}$ mice. FXR$^{-/-}$ mice were either separately transfused with the indicated adenovirus or saline alone (KO) by tail vain injection ($n = 6$ per group). After 7 days, mice were fasted for 16 h before being killed. Hepatic mRNA levels were determined by Northern blot assay (*Inset*), and plasma glucose levels were determined. *, $P < 0.05$. **, $P < 0.01$. #, $P < 0.001$ versus mice transfused with Ad-VP16.

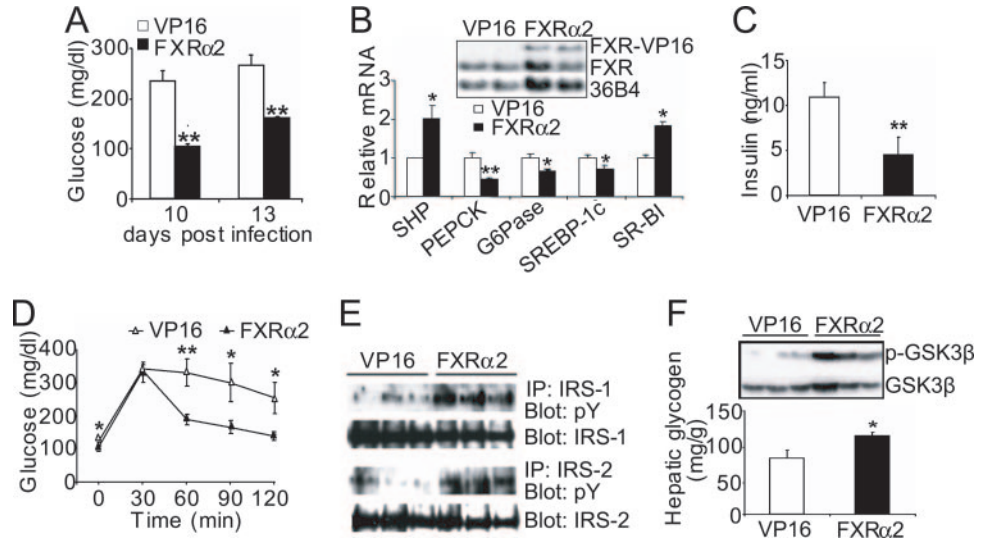

Fig. 5. Hepatic expression of FXR-VP16 significantly improves hyperglycemia in db/db mice. (*A*) Nine-week-old female db/db mice were transfused with adenovirus expressing VP16 alone (open bars) or FXRα2-VP16 (filled bars) by tail vain injection ($n = 6$ per group). Plasma glucose levels were determined after a 6-h fast on the indicated day after infection. (*B*) Hepatic mRNA levels were determined by Northern blot assay (*Inset*) or real-time PCR in db/db mice on day 13 after adenoviral injection. (*C*) Plasma insulin levels in db/db mice transfused with the indicated adenovirus were measured on day 13 after a 6-h fast. (*D*) Glucose tolerance test (GTT). db/db mice were transfused with the indicated adenovirus and, on day 7, they were fasted for 16 h before a GTT ($n = 6$ per group). (*E*) Determination of phosphotyrosine (pY) levels of hepatic IRS-1 and IRS-2. (*F*) Determination of hepatic phosphorylated GSK3β and glycogen levels. *, $P < 0.05$ and **, $P < 0.01$ versus db/db mice transfused with VP16.

whether hepatic FXR plays a major role in mediating the effect of GW4064 on glucose homeostasis in diabetic db/db mice, we infused db/db mice with either Ad-VP16 or Ad-FXRα2-VP16. As shown in Fig. 5*A*, as compared to mice infected with Ad-VP16, hepatic expression of FXRα2-VP16 markedly reduced plasma glucose levels on day 10 or day 13 after infection. Plasma-free fatty acids and β-hydroxybutyrate levels also decreased after hepatic FXRα2-VP16 expression (Fig. 8 *A* and *B*, which is published as supporting information on the PNAS web site).

The data of Fig. 5*B Inset* show that elevated hepatic FXRα2-VP16 mRNA levels were maintained 13 days after a single infusion of the adenovirus. Hepatic mRNA expression of the insulin receptor, glucose transporter 2 or 4, or insulin degrading enzyme was unaffected by FXRα2-VP16 infection (Fig. 8*C*). In contrast, FXRα2-VP16 significantly induced hepatic small heterodimer parter (SHP) and SR-BI but repressed PEPCK, G6Pase, and SREBP-1c expression (Fig. 5*B*). Because these latter changes in gene expression are very similar to those obtained after oral administration of GW4064 to db/db mice (Fig. 2*G*), we propose that activation of hepatic FXR after GW4064 treatment leads to the hypoglycemic effect in db/db mice.

Overexpression of FXRα2-VP16 also lowered plasma insulin levels (Fig. 5*C*), suggesting that activation of hepatic FXR in db/db mice improves hyperinsulinemia. We also show that, compared to controls, FXRα2-VP16 expression significantly improved glucose tolerance in db/db mice (Fig. 5*D*) and enhanced insulin secretion during GTT of the FXR-VP16 infected mice (Fig. 9, which is published as supporting information on the PNAS web site). Finally, hepatic expression of activated FXRα2-VP16 increased the phosphorylated levels of hepatic IRS-1 and IRS-2 (Fig. 5*E*), GSK3β (Fig. 5*F Inset*), and hepatic glycogen levels (Fig. 5*F*). In conclusion, these data demonstrate that activation of hepatic FXR in db/db mice increases hepatic insulin sensitivity and regulates glucose homeostasis.

GW4064 Treatment Promotes Hypoglycemia in KK-A(y) Mice. The data from wild-type, FXR$^{-/-}$, or db/db mice demonstrate that activation of FXR lowers plasma glucose levels (Figs. 1, 2, 4, and 5) and result in changes in signaling molecules involved in insulin action (Figs. 3 and 5). To extend our studies to other models of diabetes, we treated KK-A(y) mice, a second model for type 2 diabetes that results from spontaneous mutations of polygenic sources (32), with GW4064; this treatment also significantly lowered plasma glucose and hepatic G6Pase mRNA levels (Fig. 10, which is published as supporting information on the PNAS web site). Thus, the hypoglycemic effect that results from activation of FXR is seen in mice with various genetic backgrounds.

FXR$^{-/-}$ Mice Exhibit Glucose Intolerance and Insulin Resistance. Despite the fact that activation of FXR results in hypoglycemia, fasting plasma glucose levels of wild-type and FXR$^{-/-}$ mice are not significantly different (Fig. 1*C*). These data suggest that compensatory mechanisms may normalize plasma glucose levels in unchallenged FXR$^{-/-}$ mice. Therefore, we performed glucose and insulin tolerance tests on both wild-type and FXR$^{-/-}$ mice. The data show that, compared to their wild-type littermates, FXR$^{-/-}$ mice had mildly impaired glucose tolerance (Fig. 6*A*) and insulin sensitivity (Fig. 6*B*) and markedly reduced hepatic phosphorylated levels of IRS-2 (Fig. 6*C*) and IRS-1 (data not shown) in response to insulin stimulation. Thus, loss of FXR is associated with impaired hepatic insulin signaling. This conclusion is consistent with the data showing that activated FXR enhances hepatic insulin signaling.

Discussion

In the current study, we used both GW4064, a synthetic FXR-specific agonist, and adenovirus that expresses constitutively active FXR in the liver to demonstrate that activation of FXR results in both hypoglycemia and hypolipidemia. To our knowledge, the pronounced hypoglycemic effect after activation of FXR is previously uncharacterized and expands the metabolic pathways that are controlled by this nuclear receptor. In very recent studies, Staels and colleagues (33, 34) studied wild-type and FXR$^{-/-}$ mice in the absence of FXR agonists and provided evidence that FXR also plays a role in glucose metabolism under fasting/refeeding conditions.

The hypoglycemic effect after GW4064 treatment was observed in wild-type, db/db, KK-A(y), but not FXR$^{-/-}$ mice (Figs. 1, 2, and 10). Hypoglycemia was also observed when wild-type, FXR$^{-/-}$, or

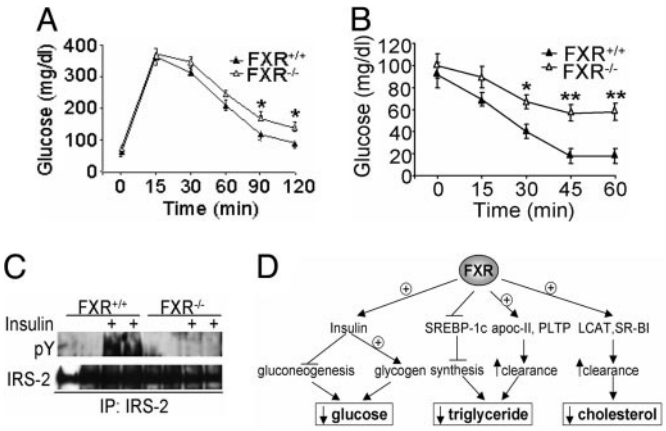

Fig. 6. A central role for FXR in glucose and lipid homeostasis. (*A* and *B*) Impaired glucose tolerance and insulin sensitivity in FXR$^{-/-}$ mice. A glucose tolerance test was performed after a 16-h fast (*A*) and insulin tolerance test (0.85 unit/kg insulin) was performed after a 5-h fast (*B*) in wild-type and FXR$^{-/-}$ mice ($n = 7$ per group). (*C*) Impaired insulin sensitivity in the liver of FXR$^{-/-}$ mice. Overnight-fasted wild-type and FXR$^{-/-}$ mice were given a bolus injection of 5 units/kg insulin or saline alone ($n = 2$ per group). After 5 min, the liver was removed and hepatic phosphotyrosine (pY) levels of IRS-2 were determined after immunoprecipitation. (*D*) Coordinate regulation of glucose and lipid metabolism by FXR in db/db mice. Activation of FXR represses hepatic gluconeogenesis and increases hepatic glycogen storage by sensitizing insulin action, resulting in decreased plasma glucose levels. Activation of FXR also lowers plasma triglyceride levels by repressing triglyceride synthesis (via repressing SREBP-1c) and increasing triglyceride clearance from blood. In addition, activation of FXR lowers plasma cholesterol levels, possibly as a result of increased SR-BI and lethithin:cholesterol acetyltransferase (LCAT) expression. *, $P < 0.05$; **, $P < 0.01$.

db/db mice were infused with adenovirus-expressing constitutively active FXR (Figs. 4 and 5). Because previous studies have shown that FXR mRNA levels are either undetectable in muscle or are expressed at very low levels in fat (12), and adenovirus infusion by tail vain injection limits expression essentially to the liver, we conclude that the hypoglycemic effect after GW4064 treatment likely results from activation of hepatic FXR.

Importantly, we show that the decrease in plasma glucose levels in db/db mice was associated with decreased G6Pase expression (Figs. 2 and 5), increased glycogen levels and synthesis in the liver (Figs. 3 and 5), and increased insulin sensitivity (Figs. 3 and 5). Consistent with these data, we demonstrate that FXR$^{-/-}$ mice exhibit impaired glucose tolerance and insulin sensitivity (Fig. 6 *A–C*). Taken together, these data demonstrate that activation of FXR lowers plasma glucose levels by sensitizing insulin action.

The effects of activated FXR on hepatic PEPCK mRNA expression depend on the genotype. For example, treatment of C57BL/6 mice with GW4064 induces hepatic PEPCK mRNA levels (Fig. 1; ref. 35), whereas the same treatment represses the enzyme in db/db mice (Figs. 2*G* and 5*B*). Diets containing 1% cholic acid, a natural FXR agonist, are reported to repress PEPCK mRNA levels by FXR-dependent (36) and FXR-independent mechanisms (37). However, comparison of these latter data with those presented herein is complicated by the finding that cholic acid-rich diets are not only hepatotoxic (13) but that this bile acid activates genes by FXR-dependent and -independent mechanisms (38). Our data, in which we identify an FXRE in the proximal PEPCK promoter and demonstrate induction of a PEPCK reporter gene by FXR (Fig. 11, which is published as supporting information on the PNAS web site) identifies PEPCK as a direct target of FXR, consistent with induction of PEPCK in C57BL/6 mice (Fig. 1). Nonetheless, in db/db mice, activation of FXR significantly increased insulin sensitivity and lowered plasma free fatty acids but decreased PEPCK expression (Figs. 3 and 5). Because PEPCK is known to be repressed after an increase in insulin sensitivity and free fatty acid levels, the data suggest that expression of PEPCK in different murine models is affected by multiple transcription factors, in addition to FXR.

Activation of FXR lowers plasma glucose levels not only in fasted mice (Figs. 1–6) but also in fed mice (Fig. 12, which is published as supporting information on the PNAS web site). Thus, the hypoglycemic effect of FXR is not restricted to fasted mice. To better understand the physiological role of FXR, we performed a pyruvate challenge by using both wild-type and FXR$^{-/-}$ mice. Plasma glucose levels were not significantly different between these two groups (Fig. 13, which is published as supporting information on the PNAS web site), suggesting that glucose production/utilization is not significantly affected in the FXR$^{-/-}$ mice. There data are consistent with our observation that the basal plasma glucose levels between wild-type and FXR$^{-/-}$ mice are similar (Figs. 1 and 6). Hyperinsulemic euglycemic clamp studies would provide additional insights into the role of FXR.

In addition to lowering plasma glucose levels, the current studies demonstrate that activated FXR also significantly lowers plasma cholesterol, triglyceride, and free fatty acid levels in wild-type and db/db (Figs. 1, 2, and 5) but not in FXR$^{-/-}$ mice (Fig. 1). The hypolipidemic effect, after activation of FXR, likely results from the repression of SREBP-1c (Figs. 1 and 5; refs. 18 and 19) and induction of genes involved in lipoprotein metabolism. Such genes include apoC-II (17), phopholipid transfer protein (PLTP) (39, 40), SR-BI (Figs. 1 and 5) and lethithin:cholesterol acetyltransferase (LCAT) (data not shown; ref. 41; Fig. 6*D*). However, the inability to induce SR-BI expression in primary hepatocytes by GW4064 treatment (data not shown) suggests that SR-BI is not a primary target gene of FXR.

Elevated circulating free fatty acids have been reported to impair the ability of insulin to stimulate glucose uptake by muscle (42). Once diabetes develops, plasma-free fatty acid levels display a linear correlation with both blood glucose levels and hepatic glucose production (43–45). Thus, the reduction in plasma-free fatty acid levels after activation of FXR (Fig. 2*D*) may contribute to increased glucose uptake by the muscle.

Numerous studies have suggested that hyperlipidemia is closely linked to cardiovascular disease. In addition, diabetes is associated with a 2- to 4-fold increase in coronary heart disease (1, 2). In view of its hypoglycemic and hypolipidemic properties, we propose that FXR agonists may be useful for treatment of diabetes and prevention of complications that include coronary heart disease.

Materials and Methods

Animals, Diets, and GW4064. C57BL/6J, Lepr$^{db/db}$ and Lepr$^{db/?}$, KK-A(y) mice from The Jackson Laboratory (Bar Harbor, ME) were fed a standard chow diet (NIH31 modified mouse/rat diet, catalog no. 7013, Harlan Teklad). Where indicated, mice were gavaged with either vehicle (2-hydroxypropyl-β-cyclodextrin, Sigma) or vehicle containing GW4064 (30 mg/kg, twice a day) for 4–11 days. Mice were fasted before they were killed as indicated in specific legends. FXR$^{-/-}$ mice on a C57BL/6 background have been characterized in ref. 13). GW4064 was kindly supplied by Patrick R. Maloney (GlaxoSmithKline) (15). All experiments were approved by the Animal Care and Research Advisory Committee at the University of California, Los Angeles.

Cell Culture. Primary hepatocytes were isolated and maintained in DMEM (25 mM glucose)/10% FBS (FBS) or 10% charcoal-stripped FBS (18).

Adenovirus. To generate adenovirus, either VP16 (the transactivation domain of herpes simplex virus) alone or murine FXRα2 cDNA (12) fused to the amino terminus of VP16 was cloned into the adenoviral vector pShuttle-IRES-hrGFP (Stratagene). After recombination in bacteria and packaging in HEK293 cells, the

resultant adenovirus was amplified in HEK293 cells, and further purified by using a BD Adeno-X Virus Purification Kit (BD Biosciences). Wild-type or $FXR^{-/-}$ mice were administered a dose of 1×10^9 plaque-forming units per mouse adenovirus by tail vain injection. After 7–13 days, mice were killed and blood and livers taken for further analysis.

Northern Blot Assay and Real-Time PCR. RNA was isolated by using TRIzol Reagent (Invitrogen). Northern blot assays were carried out by using radiolabeled probes, as indicated in ref. 12. Real-time PCR was performed on a 7700 Sequence Detector (Applied Biosystems) (12). The sequences of primers/probes are shown in *Supporting Methods*, which is published as supporting information on the PNAS web site. Results were normalized to cyclophilin or 36B4.

Quantification of Lipid, β-Hydroxybutyrate, and Insulin Levels. Plasma lipid levels were measured as described in ref. 18. Plasma β-hydroxybutyrate was measured by using an enzymatic method (Catachem, Bridgeport, CT) and plasma insulin levels determined by using an ELISA (ALPCO Diagnostics, Windham, NH).

Determination of D-Glucose Incorporation into Glycogen and Hepatic Glycogen Levels. The method to determine the incorporation of ^{14}C-D-glucose into glycogen is described in *Supporting Methods*. Hepatic glycogen was quantified by using a colorimetric assay (46).

Western Blot. Liver lysates were used for immunoprecipitation or Western blot. The detailed methods are described in *Supporting Methods*.

Liver Histology. Mouse livers were fixed in 10% neutral buffered formalin and embedded in paraffin. Sections were subjected to standard hematoxylin/eosin staining. For oil red O staining, livers were fixed in 4% parafomaldehyde in PBS, embedded in OCT, and cryosectioned. For hepatic glycogen staining, cryosections were examined by the standard periodic acid-Schiff reaction, followed by counterstaining with hematoxylin.

Glucose and Insulin Tolerance Tests. Glucose tolerance tests were performed by i.p. injection of D-glucose (Sigma) at a dose of 1.8 mg/g body weight after a 16-h fast. Insulin tolerance tests were conducted after a 5-h fast and used human regular insulin (Novolin R, Novo Nordisk) (0.85 milliunit/g body weight). Blood glucose levels were measured at the designated times by using an Onetouch Ultra glucometer (Lifescan, Mountain View, CA).

Stimulation of Insulin Signaling *in Vivo*. $FXR^{+/+}$ and $FXR^{-/-}$ mice were fasted overnight and anesthetized with pentobarbital, followed by a bolus injection with 5 units/kg of regular human insulin (Novolin R, Novo Nordisk) or saline alone, via the inferior vena cava (47). After 5 min, the liver was removed and snap frozen in liquid nitrogen. Hepatic insulin signaling molecules were assayed after immunoprecipitation.

Statistical Analysis. Results were expressed as mean ± SD. *P* values were calculated by using Student's *t* test.

This work was supported by National Institute of Health Grants HL30568 and HL68445 (to P.A.E.), a grant from the Laubisch Fund (to P.A.E.), Postdoctoral Fellowship 0325007Y from the American Heart Association (AHA) (to Y.Z.), Beginning Grant-in-Aid 0565173Y from AHA (to Y.Z.), and U.S. Public Health Service National Research Service Award GW07185 (to F.Y.L.).

1. Miettinen, H., Lehto, S., Salomaa, V., Mahonen, M., Niemela, M., Haffner, S. M., Pyorala, K. & Tuomilehto, J. (1998) *Diabetes Care* **21,** 69–75.
2. Norhammar, A., Tenerz, A., Nilsson, G., Hamsten, A., Efendic, S., Ryden, L. & Malmberg, K. (2002) *Lancet* **359,** 2140–2144.
3. The Diabetes Control and Complications Trial Research Group (1993) *N. Engl. J. Med.* **329,** 977–986.
4. UK Prospective Diabetes Study Group (1998) *Lancet* **352,** 837–853.
5. Ruderman, N. B. (1975) *Annu. Rev. Med.* **26,** 245–258.
6. Trinh, K. Y., O'Doherty, R. M., Anderson, P., Lange, A. J. & Newgard, C. B. (1998) *J. Biol. Chem.* **273,** 31615–31620.
7. Barthel, A. & Schmoll, D. (2003) *Am. J. Physiol.* **285,** E685–E692.
8. Welsh, G. I. & Proud, C. G. (1993) *Biochem. J.* **294,** 625–629.
9. Ali, A., Hoeflich, K. P. & Woodgett, J. R. (2001) *Chem. Rev.* **101,** 2527–2540.
10. Forman, B. M., Goode, E., Chen, J., Oro, A. E., Bradley, D. J., Perlmann, T., Noonan, D. J., Burka, L. T., McMorris, T., Lamph, W. W., *et al.* (1995) *Cell* **81,** 687–693.
11. Lu, T. T., Repa, J. J. & Mangelsdorf, D. J. (2001) *J. Biol. Chem.* **276,** 37735–37738.
12. Zhang, Y., Kast-Woelbern, H. R. & Edwards, P. A. (2003) *J. Biol. Chem.* **278,** 104–110.
13. Sinal, C., J., Tohkin, M., Miyata, M., Ward, J. M., Lambert, G. & Gonzalez, F. J. (2000) *Cell* **102,** 731–744.
14. Edwards, P. A., Kast, H. R. & Anisfeld, A. M. (2002) *J. Lipid Res.* **43,** 2–12.
15. Maloney, P. R., Parks, D. J., Haffner, C. D., Fivush, A. M., Chandra, G., Plunket, K. D., Creech, K. L., Moore, L. B., Wilson, J. G., Lewis, M. C., *et al.* (2000) *J. Med. Chem.* **43,** 2971–2974.
16. Holt, J. A., Luo, G., Billin, A. N., Bisi, J., McNeill, Y. Y., Kozarsky, K. F., Donahee, M., Wang da, Y., Mansfield, T. A., Kliewer, S. A., *et al.* (2003) *Genes Dev.* **17,** 1581–1591.
17. Kast, H. R., Nguyen, C. M., Sinal, C. J., Jones, S. A., Laffitte, B. A., Reue, K., Gonzalez, F. J., Willson, T. M. & Edwards, P. A. (2001) *Mol. Endocrinol.* **15,** 1720–1728.
18. Zhang, Y., Castellani, L. W., Sinal, C. J., Gonzalez, F. J. & Edwards, P. A. (2004) *Genes Dev.* **18,** 157–169.
19. Watanabe, M., Houten, S. M., Wang, L., Moschetta, A., Mangelsdorf, D. J., Heyman, R. A., Moore, D. D. & Auwerx, J. (2004) *J. Clin. Invest.* **113,** 1408–1418.
20. Goodwin, B., Jones, S. A., Price, R. R., Watson, M. A., McKee, D. D., Moore, L. B., Galardi, C., Wilson, J. G., Lewis, M. C., Roth, M. E., *et al.* (2000) *Mol. Cell.* **6,** 517–526.
21. Lu, T. T., Makishima, M., Repa, J. J., Schoonjans, K., Kerr, T. A., Auwerx, J. & Mangelsdorf, D. J. (2000) *Mol. Cell* **6,** 507–515.
22. Connelly, M. A. & Williams, D. L. (2004) *Curr. Opin. Lipidol.* **15,** 287–295.
23. Kozarsky, K. F., Donahee, M. H., Rigotti, A., Iqbal, S. N., Edelman, E. R. & Krieger, M. (1997) *Nature* **387,** 414–417.
24. Coleman, D. L. (1978) *Diabetologia* **14,** 141–148.
25. Leibel, R. L., Chung, W. K. & Chua, S. C., Jr. (1997) *J. Biol. Chem.* **272,** 31937–31940.
26. Duran-Sandoval, D., Mautino, G., Martin, G., Percevault, F., Barbier, O., Fruchart, J. C., Kuipers, F. & Staels, B. (2004) *Diabetes* **53,** 890–898.
27. Saltiel, A. R. & Kahn, C. R. (2001) *Nature* **414,** 799–806.
28. Embi, N., Rylatt, D. B. & Cohen, P. (1980) *Eur. J. Biochem.* **107,** 519–527.
29. Plyte, S. E., Hughes, K., Nikolakaki, E., Pulverer, B. J. & Woodgett, J. R. (1992) *Biochim. Biophys. Acta* **1114,** 147–162.
30. Cross, D. A., Alessi, D. R., Cohen, P., Andjelkovich, M. & Hemmings, B. A. (1995) *Nature* **378,** 785–789.
31. Virkamaki, A., Ueki, K. & Kahn, C. R. (1999) *J. Clin. Invest.* **103,** 931–943.
32. Reddi, A. S. & Camerini-Davalos, R. A. (1988) *Adv. Exp. Med. Biol.* **246,** 7–15.
33. Duran-Sandoval, D., Cariou, B., Percevault, F., Hennuyer, N., Grefhorst, A., van Dijk, T. H., Gonzalez, F. J., Fruchart, J. C., Kuipers, F. & Staels, B. (2005) *J. Biol. Chem.* **280,** 29971–29979.
34. Cariou, B., van Harmelen, K., Duran-Sandoval, D., van Dijk, T., Grefhorst, A., Bouchaert, E., Fruchart, J. C., Gonzalez, F. J., Kuipers, F. & Staels, B. (2005) *FEBS Lett.* **579,** 4076–4080.
35. Stayrook, K. R., Bramlett, K. S., Savkur, R. S., Ficorilli, J., Cook, T., Christe, M. E., Michael, L. F. & Burris, T. P. (2005) *Endocrinology* **146,** 984–991.
36. Yamagata, K., Daitoku, H., Shimamoto, Y., Matsuzaki, H., Hirota, K., Ishida, J. & Fukamizu, A. (2004) *J. Biol. Chem.* **279,** 23158–23165.
37. De Fabiani, E., Mitro, N., Gilardi, F., Caruso, D., Galli, G. & Crestani, M. (2003) *J. Biol. Chem.* **278,** 39124–39132.
38. Gupta, S., Stravitz, R. T., Dent, P. & Hylemon, P. B. (2001) *J. Biol. Chem.* **276,** 15816–15822.
39. Laffitte, B. A., Kast, H. R., Nguyen, C. M., Zavacki, A. M., Moore, D. D. & Edwards, P. A. (2000) *J. Biol. Chem.* **275,** 10638–10647.
40. Urizar, N. L., Dowhan, D. H. & Moore, D. D. (2000) *J. Biol. Chem.* **275,** 39313–39317.
41. Jonas, A. (2000) *Biochim. Biophys. Acta* **1529,** 245–256.
42. Roden, M., Price, T. B., Perseghin, G., Petersen, K. F., Rothman, D. L., Cline, G. W. & Shulman, G. I. (1996) *J. Clin. Invest.* **97,** 2859–2865.
43. Reaven, G. M. & Chen, Y. D. (1988) *Am. J. Med.* **85,** 106–112.
44. Boden, G. & Chen, X. (1995) *J. Clin. Invest.* **96,** 1261–1268.
45. Boden, G. (1999) *Proc. Assoc. Am. Physicians* **111,** 241–248.
46. Lo, S., Russell, J. C. & Taylor, A. W. (1970) *J. Appl. Physiol.* **28,** 234–236.
47. Taniguchi, C. M., Ueki, K. & Kahn, R. (2005) *J. Clin. Invest.* **115,** 718–727.